ORIGINAL

CT Radiomics of Pericoronary Fat to Predict Coronary Artery Calcification

Leah Bollos[1], Ryosuke Kasai[2], Yoichi Otomi[3], Shoichiro Takao[4], Masataka Sata[5], Masafumi Harada[3], and Hideki Otsuka[2]

[1]Graduate School of Medicine, Tokushima University, Tokushima, Japan, [2]Department of Medical Imaging/ Nuclear Medicine Institute of Biomedical Sciences, Tokushima University, Japan, Tokushima University Hospital, Tokushima, Japan, [3]Department of Radiology, Institute of Biomedical Sciences, S, Tokushima University Hospital, Japan, [4]Department of Diagnostic Radiology, Institute of Biomedical Sciences, Tokushima University, Graduate School, Tokushima, Japan, [5]Department of Cardiovascular Medicine, Tokushima University Hospital, Tokushima, Japan

Abstract : Background : Coronary artery disease (CAD) is a leading cause of mortality worldwide. Coronary artery calcification (CAC) is a key indicator of CAD, reflecting plaque burden. Pericoronary adipose tissue (PCAT) promotes vascular inflammation and contributes to plaque development, making it a promising imaging biomarker. This study aimed to create a radiomics-based model using cardiac CT features of PCAT around the left main coronary artery (LMCA) to predict CAC. Methods : Imaging from forty patients who underwent ECG-gated cardiac CT was retrospectively analyzed and grouped by CAC presence. Manual segmentation was performed using 3D Slicer to delineate PCAT surrounding the LMCA. Minimum Redundancy Maximum Relevance (mRMR) and Least Absolute Shrinkage and Selection Operator (LASSO) regression were utilized for feature selection. Random Forest and support vector machine (SVM) models were trained and compared. Results : From the 1,037 features extracted, two features with non-zero coefficients were retained at the optimal LASSO parameter (log α = 0.0128). The Random Forest model achieved 92% accuracy and an area under the curve (AUC) of 0.9143, outperforming SVM. Conclusion : Radiomic features of PCAT on cardiac CT can accurately predict CAC, showing its potential as an imaging-based biomarker for CAD risk assessment. J. Med. Invest. 72 : 330-336, August, 2025

Keywords **:** *radiomics, pericoronary adipose tissue, cardiac computed tomography, machine learning*

INTRODUCTION

Coronary artery disease (CAD) is a leading cause of global mortality and disability (1), mainly due to the progression of atherosclerotic plaques that narrow or occlude coronary arteries, leading to myocardial infarction or sudden death (2). Conventional imaging techniques such as coronary artery calcification (CAC) scoring and stenosis evaluation via coronary computed tomography angiography (CCTA) are widely employed for risk stratification. However, these approaches may fail to detect early-stage vascular inflammation or identify vulnerable plaques prone to rupture (3-5).

Growing evidence illustrates the pathophysiological role of perivascular adipose tissue (PVAT), the fat surrounding blood vessels, in modulating vascular homeostasis (5-7). Under normal physiological conditions, PVAT exerts anti-inflammatory and vasodilatory effects. However, under metabolic or oxidative stress, PVAT undergoes phenotypic switching to a pro-inflammatory state, characterized by cytokine release, oxidative stress, and altered adipokine secretion. This promotes local vascular inflammation and accelerates atherosclerosis (3, 5). In the coronary circulation, this subset of PVAT is anatomically referred to as pericoronary adipose tissue (PCAT). PCAT is anatomically positioned adjacent to the coronary wall, where it actively participates in local vascular homeostasis and inflammation (4). Under pathological conditions inflammatory remodeling, characterized by adipocyte shrinkage, fibrosis and altered lipid-water content (7), has been associated with the development and progression of coronary pathology (4-6). Increasing attention has been paid to the role of PCAT in the pathogenesis of CAD (4-6, 7). Recent reviews further highlight PCAT's potential as a noninvasive imaging biomarker for vascular inflammation and residual cardiovascular risk, supported by its close anatomical proximity to the coronary wall and dynamic radiodensity changes in response to inflammatory signaling (7, 8). CT-derived PCAT features, including radiodensity and textural metrics, have been shown to correlate with vascular inflammation (7-9) have been shown to reflect early atherovascular inflammatory activity (6-9), reflect early atherosclerotic changes, and offer added value in predicting cardiovascular risk (8).

Among coronary segments, the left main coronary artery (LMCA) holds particular clinical importance. It supplies blood to a large portion of the left ventricular myocardium and is associated with the highest risk of adverse cardiac events when diseased (10). Hemodynamic forces and shear stress patterns at the LMCA bifurcation make it especially susceptible to early

List of Abbreviations :
AUC : Area Under the Curve, CAC : Coronary Artery Calcification, CAD : Coronary Artery Disease, CCTA : Coronary Computed Tomography Angiography, CT : Computed Tomography, ECG : Electrocardiogram, FAI : Fat Attenuation Index, LASSO : Least Absolute Shrinkage and Selection Operator, LMCA : Left Main Coronary Artery, mRMR : Minimum Redundancy Maximum Relevance, PCAT : Pericoronary Adipose Tissue, PVAT : Perivascular Adipose Tissue, RF : Random Forest, ROC : Receiver Operating Characteristic, ROI : Region of Interest, SVM : Support Vector Machine

Received for publication April 24, 2025 ; accepted May 23, 2025.

Address correspondence and reprint requests to Ryosuke Kasai, Kuramoto-cho 3-18-15, Tokushima City, Tokushima, 770-8503, Japan and E-mail : kasai-r@tokushima-u.ac.jp

atherosclerotic plaque formation, which may affect prognosis (10, 11). While PCAT has been evaluated around various coronary segments, the LMCA remains a compelling target for analysis due to its prognostic significance and potential influence on vascular remodeling (12).

Cardiac computed tomography (CT), particularly CCTA, enables a non-invasive and detailed visualization of coronary anatomy and surrounding perivascular structures, including PCAT. Quantitative markers such as the fat attenuation index (FAI) derived from CT have demonstrated predictive value for coronary inflammation and stratifying coronary risk (2, 4). However, these single-value attenuation metrics do not account for the full spectrum of tissue heterogeneity (7). To address this limitation, artificial intelligence techniques such as radiomics and deep learning can detect subtle imaging patterns before overt calcification or clinical events occur. These methods can extract advanced image-based features and analyze textural and spatial variations within PCAT and coronary plaques, potentially allowing earlier detection of disease process (13, 14). Radiomic features extracted from PCAT have been shown to correlate strongly with coronary inflammation and offer improved discriminatory performance of early-stage atherosclerosis compared to traditional CT-derived metrics (15).

Radiomics-based models using cardiac CT have shown promise in identifying vulnerable plaques (7, 16), predicting CAC (17), and outperforming visual or histogram-based assessments in detecting early disease states (16, 18). Incorporating radiomics into CCTA workflows enhances objectivity and reproducibility, particularly in evaluating pericoronary fat distribution and calcification, while reducing inter-reader variability when supported using AI-supported systems (19). Early coronary plaque or calcification detection holds significant clinical implications, enabling timely intervention, risk factor modification, and better long-term outcomes (3, 20). Since obstructive events can result from non-calcified or minimally calcified plaques, characterizing the perivascular microenvironment may provide additional diagnostic value beyond traditional measures (3, 21).

Despite these advantages, radiomics must also be evaluated in context with other modalities that offer complementary strengths and limitations. While invasive modalities such as intravascular ultrasound and optical coherence tomography provide detailed plaque visualization, and PET/CT assesses metabolic activity, they are less practical for widespread screening (11, 18). In contrast, radiomics applied to cardiac CT represents a scalable, non-invasive tool for personalized risk stratification and atherosclerotic disease monitoring (9, 13, 18).

To focus on this potential, this study developed a radiomics-based prediction model for CAC using features extracted from PCAT surrounding the left main coronary artery on ECG-gated cardiac CT. By focusing on this high-risk region, we aimed to evaluate whether PCAT characteristics from CT imaging can effectively predict calcification and potentially support risk assessment in CAD in the future.

PATIENTS AND METHODS

This retrospective study analyzed the imaging data of 40 patients who underwent ECG-gated CCT at Tokushima University Hospital. The imaging data was categorized into two groups based on the presence or absence of CAC, as assessed through CT imaging. Imaging from 20 patients demonstrated coronary calcification (calcification group), while the remaining 20 had no observable calcified plaques, with a calcium score of zero (non-calcification group). All image data were anonymized and processed following institutional data protection protocols.

Image Acquisition and Segmentation

Using the SYNAPSE Vincent workstation (Fujifilm), coronary CT images were acquired using a standard ECG-gated protocol optimized for coronary artery visualization. The perivascular region around the left main coronary artery was identified and images were exported in DICOM format. The formatted images were processed using the Segment Editor module in 3D Slicer (version 5.2.2), an open-source image analysis platform (22). The level- tracing tool was used to manually delineate PCAT surrounding the LMCA. Segmentation was performed across 30 consecutive slices, covering a longitudinal segment of 10-50 mm distal to the LMCA ostium. An example of the segmentation process and resulting region of interest (ROI) is shown in Figure 1.

Preprocessing Parameters and Feature Extraction

To ensure consistency across patient images, the following preprocessing settings were applied :

1. Image normalization : A CT images were normalized to a range of 0 to 1 prior to feature extraction to mitigate variability due to absolute intensity differences.
2. Intensity discretization was performed using a fixed bin width of 27, dividing the 0-1 range into approximately 37 bins. This value was chosen based on preliminary testing to balance feature robustness and sensitivity.
3. Resampling : No resampling was applied ; the original voxel spacing was preserved throughout the feature extraction process.
4. Interpolation : B-spline interpolation (sitkBSpline) was used during mask processing to preserve anatomical accuracy and ensure smooth boundary transitions.

Feature extraction was performed independently for each subject prior to any data splitting. That is, all Radiomics features were extracted from the original images before separating the dataset into training and test cohorts. To avoid data leakage, feature selection and model training were performed exclusively on the training cohort, without using any information from the test cohort. The test cohort was strictly held out and used only for final model evaluation and at no point were test data involved in feature selection, model optimization, or parameter tuning.

Radiomic Analysis and Feature Selection

Following segmentation, radiomic features were extracted from each PCAT region utilizing a two-step feature selection process was performed to reduce dimensionality and eliminate redundancy. The Minimum Redundancy Maximum Relevance (mRMR) algorithm (23) was first applied to prioritize features with the highest relevance to the classification task. This was followed by Least Absolute Shrinkage and Selection Operator (LASSO) regression (24) to further refine the feature set, selecting only those with non-zero coefficients for model construction.

Model Development

The dataset was randomly split into a training set (n = 28) and a test set (n = 12) using a 7 : 3 ratio. The Random Forest and Support Vector Machine (SVM) algorithms were respectively developed to distinguish between patients with and without CAC. Model training and testing were repeated across multiple randomized shuffles to ensure stability and robustness.

Performance Evaluation

Random Forest and SVM classifiers were trained and tested across multiple randomized splits. Classification accuracy was compared between the two models, and the better-performing model was selected for final performance evaluation, including ROC analysis and feature importance assessment.

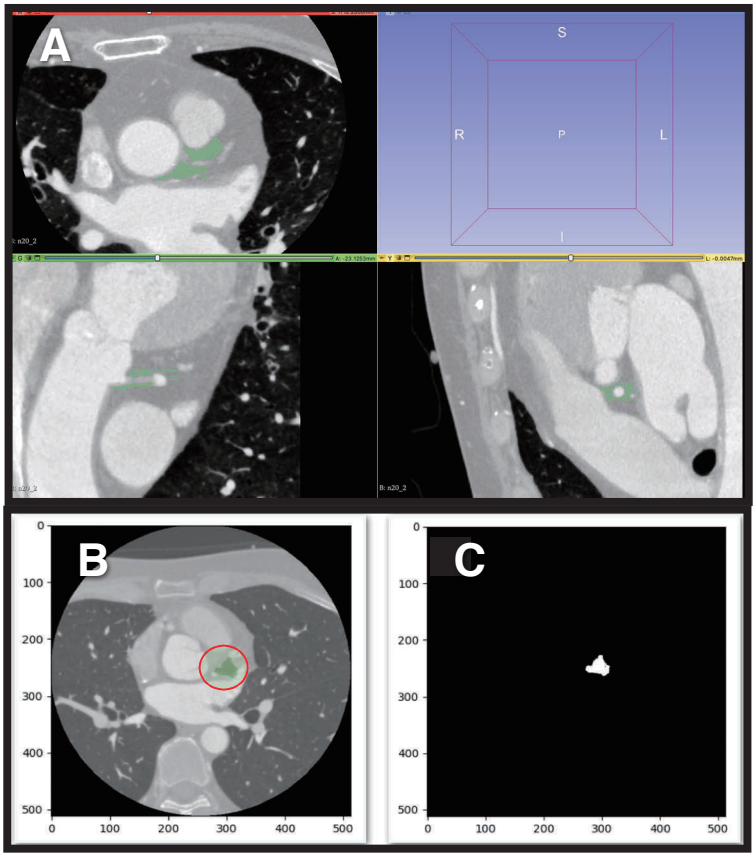

Figure 1. Example of pericoronary adipose tissue segmentation around the left main coronary artery
(A) shows the 3D Slicer interface displaying the cardiac CT scan in axial, coronal, and sagittal views during manual segmentation. (B) displays an axial slice with the PCAT region highlighted in green and marked by a red circle. (C) shows the corresponding binary mask of the segmented region of interest (ROI) used for radiomic feature extraction.
Abbreviations : PCAT, pericoronary adipose tissue ; LMCA, left main coronary artery ; CT, computed tomography ; ROI, region of interest.

RESULTS

Of the 1,037 radiomic features initially extracted from pericoronary adipose tissue, two features were retained after mRMR and LASSO regression processing. The two features with non-zero coefficients at the optimal regularization parameter (log α = 0.0128) were Wavelet-HHL_firstorder_Minimum and Wavelet-HHH_firstorder_Minimum. These features represent first-order minimum intensity values in high-frequency wavelet-transformed image components and are shown to capture fine-scale variations in tissue density. The distribution of all radiomic features across patients is visualized in Figure 2.

Using the selected features, classification models were developed with both Random Forest and SVM algorithms. The Random Forest model achieved a classification accuracy of 92%, outperforming the SVM, which reached 83% accuracy. As a result, Random Forest was selected for final evaluation. Feature selection results, including the regularization path and cross-validation output, are illustrated in Figure 3. These visualizations confirm the robustness of the selected features.

Receiver Operating Characteristic (ROC) curve analysis of the Random Forest classifier yielded an Area Under the Curve (AUC) of 0.9143, demonstrating high discriminative performance in distinguishing patients with and without CAC (Figure 4).

DISCUSSION

This study developed a radiomics-based prediction model using PCAT features on cardiac CT to predict CAC. Among 1,037 extracted features, two wavelet-transformed first-order features were retained after selection, and the Random Forest classifier achieved an AUC of 0.9143, demonstrating strong discriminatory capability.

The AUC achieved in this study is notably higher than those reported in prior PCAT radiomics studies predicting CAC or coronary inflammation, such as Hu *et al*. (17), who reported an AUC of 0.846 using a combined clinical and radiomics model, or Cheng *et al*. (15), who reported AUCs in the 0.8–0.88 range for coronary inflammation detection. This suggests that our selected features—though fewer in number—may capture meaningful pathological variation in pericoronary adipose tissue, particularly in the LMCA region.

Understanding how PCAT morphology reflects underlying coronary pathology is essential for interpreting the biological significance of radiomics features retained in predictive models. Radiomics enables the extraction of quantitative tissue characteristics that go beyond visual interpretation. Prior studies have demonstrated that inflammatory modeling of PCAT, including adipocyte shrinkage, fibrotic expansion, immune cell infiltration, and altered microvascular architecture, contributes to heterogeneity in CT attenuation values (4, 6, 17). These subtle

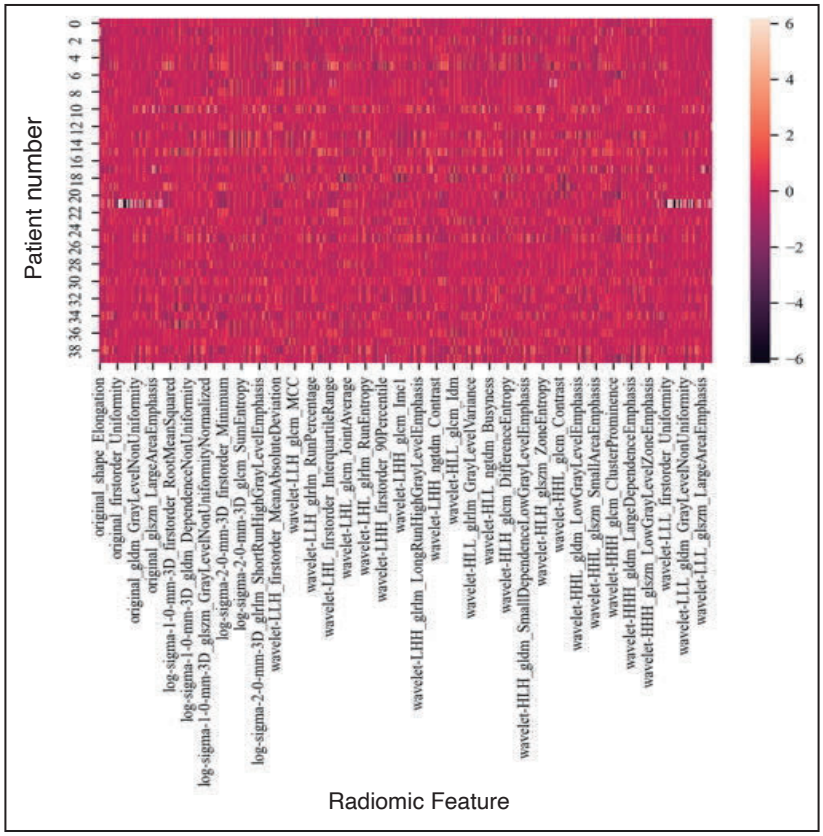

Figure 2. Heatmap of normalized radiomic features extracted PCAT
This heatmap displays the distribution of 1,037 radiomic features across 40 patients, with y-axis corresponding to individual patients and x-axis representing individual features. Patients 0–19 represent the calcification group, while patients 20–39 represent the non-calcification group. Feature values were normalized for visualization. Because group-wise clustering is not visually apparent, machine learning is required to extract and interpret discriminative patterns from the data.
Abbreviations : PCAT, pericoronary adipose tissue ; CAC, coronary artery calcification.

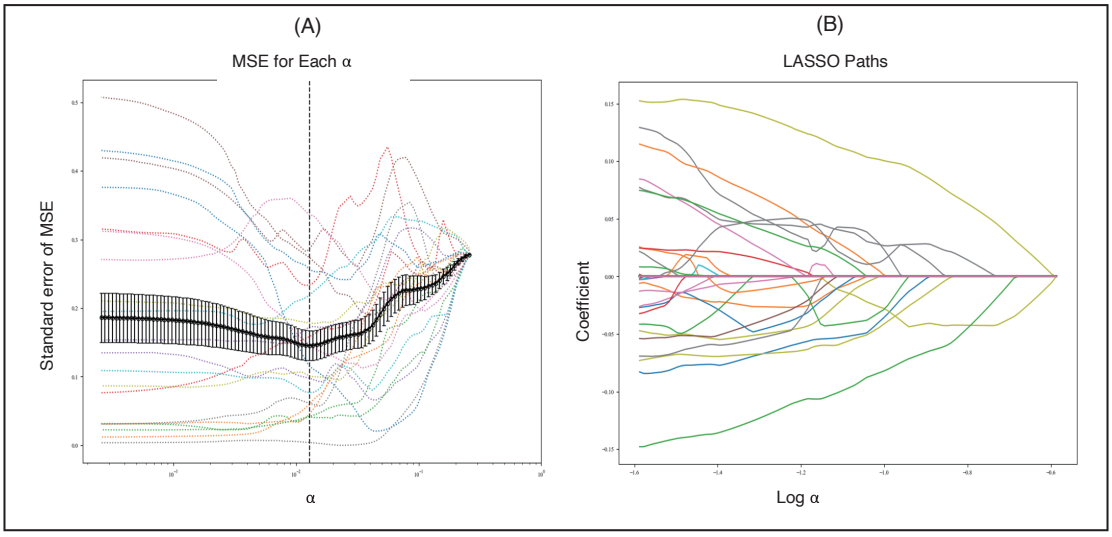

Figure 3. Feature selection using LASSO regression.
(A) shows the 10-fold cross-validation used to find the best regularization value (log α = 0.0128). The x-axis shows the log-transformed α values, and the y-axis shows mean squared error (MSE), which measures how well the model predictions match the actual outcomes. Each colored line represents the MSE across folds in the cross-validation. The solid curve denotes the average MSE. The minimum point on the curve identifies the α that minimizes prediction error. (B) represents how the 40 radiomic feature coefficients change as α increases. Each colored line corresponds to one radiomic feature. As α increases, most features are progressively shrunk toward zero. Two features (Wavelet-HHL_firstorder_Minimum and Wavelet-HHH_firstorder_Minimum) remained at the optimal α and were selected for model building.
Abbreviations : LASSO, least absolute shrinkage and selection operator ; α, regularization parameter ; HHL/HHH, high-frequency wavelet decomposition components along the x-, y-, and z-axes ; mRMR, minimum redundancy maximum relevance.

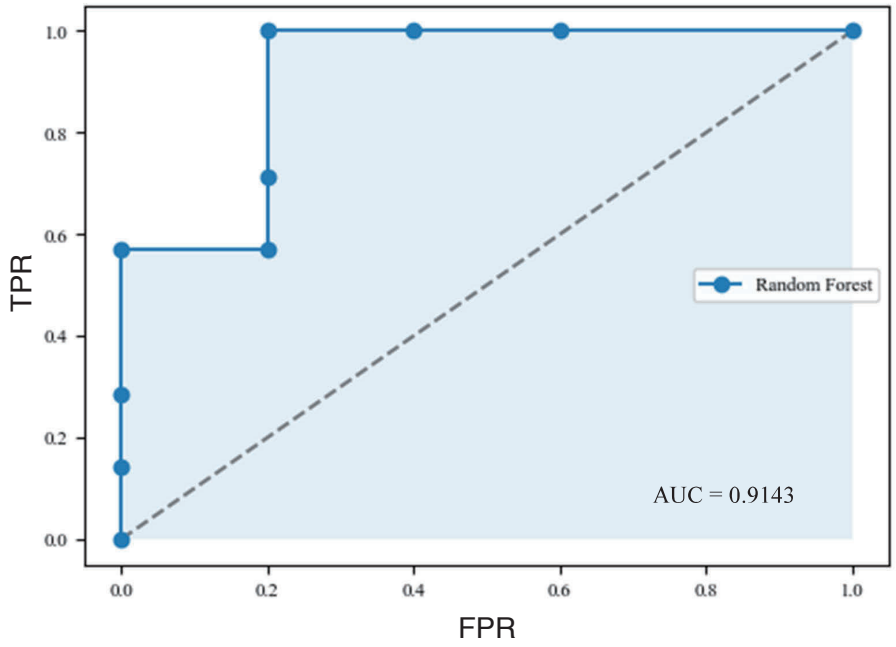

Figure 4. Receiver Operating Characteristic (ROC) curve of the Random Forest model.
The ROC curve illustrates the model's discriminative ability in classifying patients with and without CAC. The AUC was 0.9143, indicating high classification performance.
Abbreviations : ROC, receiver operating characteristic ; AUC, area under the curve ; CAC, coronary artery calcification TPR, true positive rate ; FPR false positive rate.

changes may not be fully captured by simplified metrics such as the FAI, which reduces tissue complexity to a single mean value (8, 15).

Wavelet-transformed features break the CT image into multiple resolution levels to detect fine textural variations, while first-order descriptors measure how voxel intensities are distributed, reflecting tissue heterogeneity (13, 15). These radiomic attributes particularly sensitive to inflammatory and fibrotic remodeling (8, 15). Tan *et al*. (7) further notes that the PCAT remodeling in response to inflammation may influence CT signals even in the absence of overt plaques, supporting radiomics' capacity to detect subclinical disease processes.

Our anatomical focus on the left main coronary artery (LMCA) enhances clinical relevance of this model. The LMCA perfuses a large myocardial territory and is associated with a higher risk of adverse cardiac outcomes (11). Its bifurcation and hemodynamic profile make it particularly prone to early atherogenensis. Previous work, such as Hu *et al*. (17), has demonstrated that PCAT radiomic features near the LMCA are discriminative of calcified plaques. Evaluating PCAT in this segment may therefore yield localized radiomic signatures not apparent in global scoring systems.

In addition, our findings align with research by Militello *et al*. (16), who demonstrated that combining radiomic features with clinical biomarkers improved CAD prediction and interpretability in their multimodal model. Although our model was built using imaging data alone, its high internal performance emphasizes the diagnostic potential of PCAT radiomics as a non-invasive imaging biomarker.

While promising, radiomics still faces challenges in clinical application. Differences in acquisition protocols, segmentation methods, and feature extraction pipelines contribute to variability. As emphasized by Motwani *et al*. (25), standardization, multicenter validation, and integration of clinical parameters are necessary for broader applicability. Radiomics should not be viewed in isolation : cardiovascular risk is multifactorial, and while only a few clinical variables such as age and lipid profile correlate strongly with CAC (16), integrating clinical and imaging data could improve model interpretability and support more personalized decision-making.

This study has several limitations. The sample size was relatively small and derived from a single center, which may limit generalizability. Stratified modeling based on CAC severity (e.g., mild, moderate, severe) was not feasible due to the sample size. Furthermore, histopathological correlation was not performed, though our findings are consistent with prior imaging-pathology studies (6-8). Future work should include larger, diverse populations and explore combined modeling with clinical variables to improve interpretability and personalized risk assessment.

CONCLUSION

This study demonstrated that radiomic features extracted from pericoronary adipose tissue surrounding the left main coronary artery on ECG-gated coronary CT can effectively predict coronary artery calcification. The model's strong performance highlights the potential of PCAT radiomics as a non-invasive imaging marker for early coronary pathology. Further validation in larger, multi-center cohorts is warranted to confirm its clinical utility.

CONFLICT OF INTEREST

The authors declare no conflict of interest.

ACKNOWLEDGEMENTS

The authors express their gratitude to Tokushima University Hospital for providing the imaging data used in this article. In addition, the Otsuka Toshimi Scholarship Foundation is acknowledged for its support of Dr. Leah Bollos.

ETHICS APPROVAL

This study was approved by the Ethics Committee of Tokushima University Hospital (approval number : 4295-3).

REFERENCES

1. Martin SS, Aday AW, Almarzooq ZI, Anderson CAM, Arora P, Avery CL, Baker-Smith CM, Barone Gibbs B, Beaton AZ, Boehme AK, Commodore-Mensah Y, Currie ME, Elkind MSV, Evenson KR, Generoso G, Heard DG, Hiremath S, Johansen MC, Kalani R, Kazi DS, Ko D, Liu J, Magnani JW, Michos ED, Mussolino ME, Navaneethan SD, Parikh NI, Perman SM, Poudel R, Rezk-Hanna M, Roth GA, Shah NS, St-Onge MP, Thacker EL, Tsao CW, Urbut SM, Van Spall HGC, Voeks JH, Wang NY, Wong ND, Wong SS, Yaffe K, Palaniappan LP : 2024 Heart disease and stroke statistics : A report of US and global data from the American Heart Association. Circulation 149 : e347-e913, 2024. doi : 10.1161/CIR.0000000000001209
2. Greenland P, Blaha MJ, Budoff MJ, Erbel R, Watson KE : Coronary calcium score and cardiovascular risk. Journal of the American College of Cardiology 72(4) : 434-47, 2018. https://doi.org/10.1016/j.jacc.2018.05.027.
3. Dweck MR, Loganath K : Coronary plaque and the adjacent fat. JACC : Cardiovascular Imaging 15(10) : 1768-70, 2022. https://doi.org/10.1016/j.jcmg.2022.06.016.
4. Wang J, Zhang H, Wang Z, Liu W, Cao D, Tong Q : Evaluating the role of pericoronary adipose tissue on coronary artery disease : insights from CCTA on risk assessment, vascular stenosis, and plaque characteristics. Frontiers in Cardiovascular Medicine 11 : 1451807, 2024
5. Lee S-E, Sung JM, Andreini D, Al-Mallah MH, Budoff MJ, Cademartiri F, Chinnaiyan K, Choi JH, Chun EJ, Conte E, Gottlieb I, Hadamitzky M, Kim YJ, Lee BK, Leipsic JA, Maffei E, Marques H, De Araújo Gonçalves P, Pontone G, Shin S, Kitslaar PH, Reiber JHC, Stone PH, Samady H, Virmani R, Narula J, Berman DS, Shaw LJ, Bax JJ, Lin FY, Min JK, Chang H-J : Association between changes in perivascular adipose tissue density and plaque progression. JACC : Cardiovascular Imaging 15(10) : 1760-7, 2022. https://doi.org/10.1016/j.jcmg.2022.04.016.5.
6. Antonopoulos AS, Sanna F, Sabharwal N, Thomas S, Oikonomou EK, Herdman L, Margaritis M, Shirodaria C, Kampoli A-M, Akoumianakis I, Petrou M, Sayeed R, Krasopoulos G, Psarros C, Ciccone P, Brophy CM, Digby J, Kelion A, Uberoi R, Anthony S, Alexopoulos N, Tousoulis D, Achenbach S, Neubauer S, Channon KM, Antoniades C : Detecting human coronary inflammation by imaging perivascular fat. Sci Transl Med 9(398) : eaal2658, 2017. https://doi.org/10.1126/scitranslmed.aal2658.
7. Tan N, Dey D, Marwick TH, Nerlekar N : Pericoronary Adipose Tissue as a Marker of Cardiovascular Risk : JACC review topic of the week. Journal of the American College of Cardiology 81 : 913-923, 2023
8. Oikonomou EK, Williams MC, Kotanidis CP, Desai MY, Marwan M, Antonopoulos AS, Thomas KE, Thomas S, Akoumianakis I, Fan LM, Kesavan S, Herdman L, Alashi A, Centeno EH, Lyasheva M, Griffin BP, Flamm SD, Shirodaria C, Sabharwal N, Kelion A, Dweck MR, Van Beek EJR, Deanfield J, Hopewell JC, Neubauer S, Channon KM, Achenbach S, Newby DE, Antoniades C : A novel machine learning-derived radiotranscriptomic signature of perivascular fat improves cardiac risk prediction using coronary CT angiography. European Heart Journal 40(43) : 3529-43, 2019. https://doi.org/10.1093/eurheartj/ehz592.
9. Hirata Y, Kurobe H, Akaike M, Chikugo F, Hori T, Bando Y, Nishio C, Higashida M, Nakaya Y, Kitagawa T, Sata M : enhanced inflammation in epicardial fat in patients with coronary artery disease. International Heart Journal 52 : 139-142, 2011
10. Khawaja M, Britt M, Khan MA, Munaf U, Arshad H, Siddiqui R, Virk HUH, Alam M, Krittanawong C : Left main coronary artery disease : A contemporary review of diagnosis and management. Reviews in Cardiovascular Medicine 25(2) : 66, 2024. https://doi.org/10.31083/j.rcm2502066.
11. Voros S, Rinehart S, Qian Z, Joshi P, Vazquez G, Fischer C, Belur P, Hulten E, Villines TC : Coronary atherosclerosis imaging by coronary CT angiography. JACC : Cardiovascular Imaging 4(5) : 537-48, 2011. https://doi.org/10.1016/j.jcmg.2011.03.006.
12. Wang J, Zhang H, Wang Z, Liu W, Cao D, Tong Q : Evaluating the role of pericoronary adipose tissue on coronary artery disease : insights from CCTA on risk assessment, vascular stenosis, and plaque characteristics. Frontiers in Cardiovascular Medicine 11 : 1451807, 2024
13. Tatsugami F, Nakaura T, Yanagawa M, Fujita S, Kamagata K, Ito R, Kawamura M, Fushimi Y, Ueda D, Matsui Y, Yamada A, Fujima N, Fujioka T, Nozaki T, Tsuboyama T, Hirata K, Naganawa S : Recent advances in artificial intelligence for cardiac CT : Enhancing diagnosis and prognosis prediction. Diagnostic and Interventional Imaging 104(11) : 521-8, 2023. https://doi.org/10.1016/j.diii.2023.06.011.
14. Commandeur F, Goeller M, Dey D : Cardiac CT : Technological advances in hardware, software, and machine learning applications. Curr Cardiovasc Imaging Rep 11 : 19, 2018. https://doi.org/10.1007/s12410-018-9459-z.
15. Cheng K, Lin A, Yuvaraj J, Nicholls SJ, Wong DTL : Cardiac Computed Tomography Radiomics for the Non-Invasive Assessment of Coronary Inflammation. Cells 10(4) : 879, 2021. https://doi.org/10.3390/cells10040879.
16. Militello C, Prinzi F, Sollami G, Rundo L, La Grutta L, Vitabile S : CT radiomic features and clinical biomarkers for predicting coronary artery disease. Cogn Comput 15(1) : 238-53, 2023. https://doi.org/10.1007/s12559-023-10118-7.
17. Hu G, Ge Y, Hu X, Wei W : Predicting coronary artery calcified plaques using perivascular fat CT radiomics features and clinical risk factors. BMC Med Imaging 22(1) : 134, 2022. https://doi.org/10.1186/s12880-022-00858-7.
18. Gudigar A, Nayak S, Samanth J, Raghavendra U, A J A, Barua PD, Hasan MN, Ciaccio EJ, Tan R-S, Rajendra Acharya U : Recent trends in artificial intelligence-assisted coronary atherosclerotic plaque characterization. Int J Environ Res Public Health 18(19) : 10003, 2021. https://doi.org/10.3390/ijerph181910003.
19. Jiang B, Guo N, Ge Y, Zhang L, Oudkerk M, Xie X : Development and application of artificial intelligence in cardiac imaging. The British Journal of Radiology 93(1113) : 20190812, 2020. https://doi.org/10.1259/bjr.20190812.
20. Li Z, Huang H, Zhang W, Wang M, Fu G : [Prognosis of patients with vulnerable plaques indicated by coronary CT angiography]. Zhejiang Da Xue Xue Bao Yi

Xue Ban 49(1) : 76-81, 2020. https://doi.org/10.3785/j.issn.1008-9292.2020.02.07.

21. Dey D, Commandeur F : Radiomics to identify high-risk atherosclerotic plaque from computed tomography : The power of quantification. Circ : Cardiovascular Imaging 10(12) : e007254, 2017. https://doi.org/10.1161/CIRCIMAGING.117.007254.
22. Fedorov A, Beichel R, Kalpathy-Cramer J, Finet J, Fillion-Robin J-C, Pujol S, Bauer C, Jennings D, Fennessy F, Sonka M, Buatti J, Aylward S, Miller JV, Pieper S, Kikinis R : 3D Slicer as an image computing platform for the quantitative imaging network. Magnetic Resonance Imaging 30(9) : 1323-41, 2012. https://doi.org/10.1016/j.mri.2012.05.001.
23. Peng H, Long F, Ding C : Feature selection based on mutual information criteria of max-dependency, max-relevance, and min-redundancy. IEEE Transactions on Pattern Analysis and Machine Intelligence 27(8) : 1226-1238, 2005. https://doi.org/10.1109/TPAMI.2005.159.
24. Tibshirani R : Regression shrinkage and selection via the lasso. Journal of the Royal Statistical Society : Series B (Methodological) 58(1) : 267-288, 1996. https://doi.org/10.1111/j.2517-6161.1996.tb02080.x.
25. Motwani M, Dey D, Berman DS, Germano G, Achenbach S, Al-Mallah MH, Andreini D, Budoff MJ, Cademartiri F, Callister TQ, Chang H-J, Chinnaiyan K, Chow BJW, Cury RC, Delago A, Gomez M, Gransar H, Hadamitzky M, Hausleiter J, Hindoyan N, Feuchtner G, Kaufmann PA, Kim Y-J, Leipsic J, Lin FY, Maffei E, Marques H, Pontone G, Raff G, Rubinshtein R, Shaw LJ, Stehli J, Villines TC, Dunning A, Min JK, Slomka PJ : Machine learning for prediction of all-cause mortality in patients with suspected coronary artery disease : a 5-year multicentre prospective registry analysis. Eur Heart J 38(7) : 500-7, 2017. https://doi.org/10.1093/eurheartj/ehw188.